Convention Special Issue - 2019

J. Indian Chem. Soc.,
Vol. 96, October 2019, pp. 1279-1285

An *ortho*-hydroxy-arylimine based probe: Fluorescence sensitivity towards Zn^{2+} ion†

Sunanda Dey[a], Pallab Gayen[b] and Chittaranjan Sinha*[a]

[a]Department of Chemistry, Jadavpur University, Kolkata-700 032, India

E-mail: crsjuchem@gmail.com

[b]Department of Chemistry, Raja Peary Mohan College, Uttarpara-712 258, Hooghly, West Bengal, India

Manuscript received online 15 September 2019, accepted 19 September 2019

A probe 6,6′-((1*Z*,1′*Z*)-(((propane-1,3-diylbis(oxy))bis(2,1-phenylene))bis(azanylylidene))bis-(methanylylidene))bis(2-ethoxyphenol) (**H_2L**), is synthesized by the condensation of 2,2′-(propane-1,2-diylbis(oxy))dianiline with 3-ethoxy-2-hydroxy-benzaldehyde and characterized by various spectroscopic techniques (^{1}H NMR, FT-IR, ESI-MS etc.), exhibits greenish yellow emission (λ_{em} 556 nm) upon binding with Zn^{2+} ion in H_2O-CH_3CN (1:9 v/v, HEPES buffer, pH 7.4) in a mixture of seventeen other biologically important metal ions. The limit of detection (LOD) is 15.5 nM. The 1:1 composition of the complex, Zn^{2+}: L^{2-}, is supported by Job's plot, ESI-MS and ^{1}H NMR measurements.

Keywords: Zn^{2+} emission, turn-ON sensor, LOD 15.5 nM, fluorescent technique, 1:1 complexation.

Introduction

Uses of fluorescent probes for the trace/ultratrace detection of ions have been used widely in environmental monitoring and in biological studies due to high sensitivity, non-destructive nature and rapid response[1–3]. For sensing of Zn^{2+}, Al^{3+}, Cu^{2+}, Fe^{3+}, Cr^{3+}, Pd^{2+} halides, sulphide (S^{2-}), sulphite (SO_3^{2-}), pH etc. fluorescent chemosensor has been found to be very much effective[4,5]. After iron, zinc is the second most abundant transition metal ion in human body and a healthy human body contains 200 to 300 mg of zinc and plays a vital role in enzyme regulation, gene expression, neural signal transmission, apoptosis, cellular metabolism etc.[6,7]. Besides, zinc is mostly trapped inside proteins, as a structural or catalytic cofactor[8–10]. However, excess zinc in human body has responsible for many adverse effects such as ischemic stroke, Alzheimer's disease, epilepsy, Parkinson's disease, infantile diarrhea etc.[11–14]. In drinking water, the allowable limit of Zn is 76 μM (WHO recommended)[15]. Not only water but soil microbial activity in the environment also disrupted by excess zinc[16]. Since Zn^{2+} is a d^{10} configuration and is poor in spectroscopic response, hence, it is of great interest to develop a new chemosensor with high selectivity and sensitivity to Zn^{2+} ion.

Admirable detection techniques are the mass spectrometry (MS), atomic absorption spectroscopy (AAS), atomic emission spectroscopy (AES), inductively coupled plasma (ICP), electrochemical methods, fluorometry, voltammetry etc. Among this variety of methods fluorescent skills have attracted more attention[17–20]. Schiff base, a class of chelating compounds, has been commonly used as chemical probes due to simplistic synthesis, stability in wide-ranging pH, solubility in polar and mixed-polar media as well as impressive photophysical properties[21–24]. Herein, we report a new Schiff base, 6,6′-((1*Z*,1′*Z*)-(((propane-1,3-diylbis(oxy))bis(2,1-phenylene))bis(azanylylidene))bis-(methanylylidene))bis(2-ethoxyphenol) (**H_2L**) synthesized by condensation of 2,2′-(propane-1,2-diylbis(oxy))dianiline and 3-ethoxy-2-hydroxy-benzaldehyde which exhibits recognition of Zn^{2+} ion via "OFF-ON" fluorescence mechanism. The composition of **H_2L-**Zn^{2+} has been supported by some spectroscopic techniques (ESI-MS, Job's plot etc.).

Experimental

Materials and methods

The reagents required for this work were collected from Sigma-Aldrich and used without further purification. Solvents

†**Invited Lecture.**

were bought from Merck. Methanol was dried by the previously reported method[25]. The aqueous solutions were prepared using Milli-Q (Millipore) water. The metal ion solutions were prepared from their corresponding acetate/chloride or nitrate salts. ^{1}H NMR spectra were recorded on a Bruker (AC) 400 MHz FT-NMR spectrometer and the chemical shifts are stated in ppm with TMS as an internal standard. IR spectra were obtained using Perkin-Elmer LX-1 FTIR spectrophotometer with KBr pellets (4000–400 cm^{-1}). The mass spectra were recorded from a Water HRMS spectrometer with model number XEVO-G2QTOF#YCA351. Using Perkin-Elmer Lambda 25 spectrophotometer the UV-Vis spectra were recorded and the fluorescence spectra were obtained from Perkin-Elmer spectrofluorimeter of model LS55.

Synthesis of probe, H_2L

2,2′-(Propane-1,2-diylbis(oxy))dianiline (0.258 g, 1.0 mmol) and 3-ethoxy-2-hydroxy-benzaldehyde (0.332 g, 2.0 mmol) were stirred for 6 h in dry methanol solution. A clear orange coloured solution was obtained and orange needle crystals were isolated after slow evaporation. Yield: 77%. m.p.: 89°C. Microanalytical data: $C_{33}H_{34}N_2O_6$ Calcd. (Found): C, 71.46 (71.39); H, 6.18 (6.21); N, 5.05 (5.11)%; ^{1}H NMR (400 MHz, DMSO-d_6): 14.20 (s, 2H, phenolic-OH), 8.93 (s, 2H, imine-H), 6.82–7.44 (14H, aromatic-H), 4.28 (t, 4H, -CH_2-CH_2-CH_2-), 4.04 (q, 4H, -OCH_2-CH_3), 2.24 (2H, -CH_2-CH_2-CH_2-), 1.31 (t, 6H, -OCH_2-CH_3) (Fig. 1); ^{13}C NMR (400 MHz, DMSO-d_6): 162.27, 151.85, 151.74, 147.18, 135.91, 128.10, 124.07, 120.97, 119.21, 118.93, 117.98, 116.97, 113.35, 64.89, 64.34, 28.81, 14.72 (ESI†, Fig. S1); the mass spectral peak of **H_2L** was appeared at 555.27 (base peak) which corresponds to **H_2L** + H$^+$ ion (*m/z* Calcd. 555.24) and a small peak at 577.26 indicates **H_2L** + Na$^+$ ion (*m/z* Calcd. 577.23) (ESI†, Fig. S2); IR: 3370 cm^{-1} (phenolic-OH), 1619 cm^{-1} (imines C=N) (ESI†, Fig. S3).

Preparation of [ZnL]

To 10 mL MeOH solution of **H_2L** (0.30 g, 1 mmol), 10 mL MeOH solution of $Zn(OAc)_2.2H_2O$ (0.21 g, 1 mmol) was added and stirred for 6 h then the resulting solution was allowed to evaporate slowly in air. After few days a yellow crystalline product was obtained and processed for characterization. ^{1}H NMR (400 MHz, DMSO-d_6): 8.90 (s, 2H, imine-H), 6.71–7.38 (14H, aromatic-H), 4.22–4.37 (m, 8H, -CH_2-CH_2-CH_2- and -OCH_2-CH_3), 2.26 (2H, -CH_2-CH_2-CH_2-), 1.26 (t, 6H, -OCH_2-CH_3) (Fig. 1); the mass spectral peak of **H_2L**-Zn^{2+} complex was appeared at 617.22 which corresponds to Zn**L** + H$^+$ ion (*m/z* Calcd. 617.15) and a base peak at 639.20 indicates Zn**L** + Na$^+$ ion (*m/z* Calcd. 639.14) (ESI†, Fig. S4); IR: 1612 cm^{-1} (imines C=N) (ESI†, Fig. S5).

General method for UV-Vis and fluorescence studies

1.0 mM stock solutions of the various metal ions were prepared by dissolving the required amount of metal salts in Millipore water. Stock solution of the probe (1.0 mM), was prepared in CH_3CN and 100 μL of this solution was diluted using 1.9 ml CH_3CN-H_2O (v/v 9:1) containing HEPES buffer (pH 7.4), then the total volume of the solution becomes 2.0 ml and the solution concentration becomes 50 μM. 100 μL metal salt solutions were transferred to the probe solution. The absorption and emission spectra were recorded at room temperature and the excitation wavelength used for fluorescence study was 400 nm.

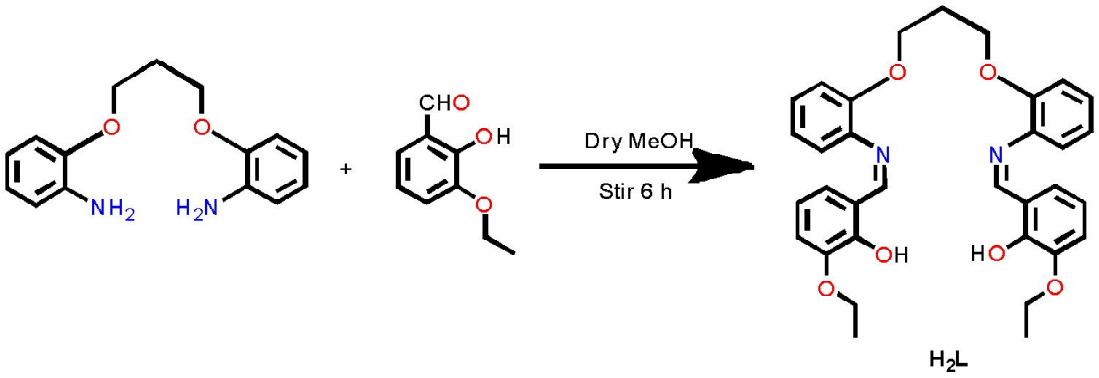

Scheme 1. Synthesis of the probe, **H_2L**.

†Electronic supplementary information (ESI).

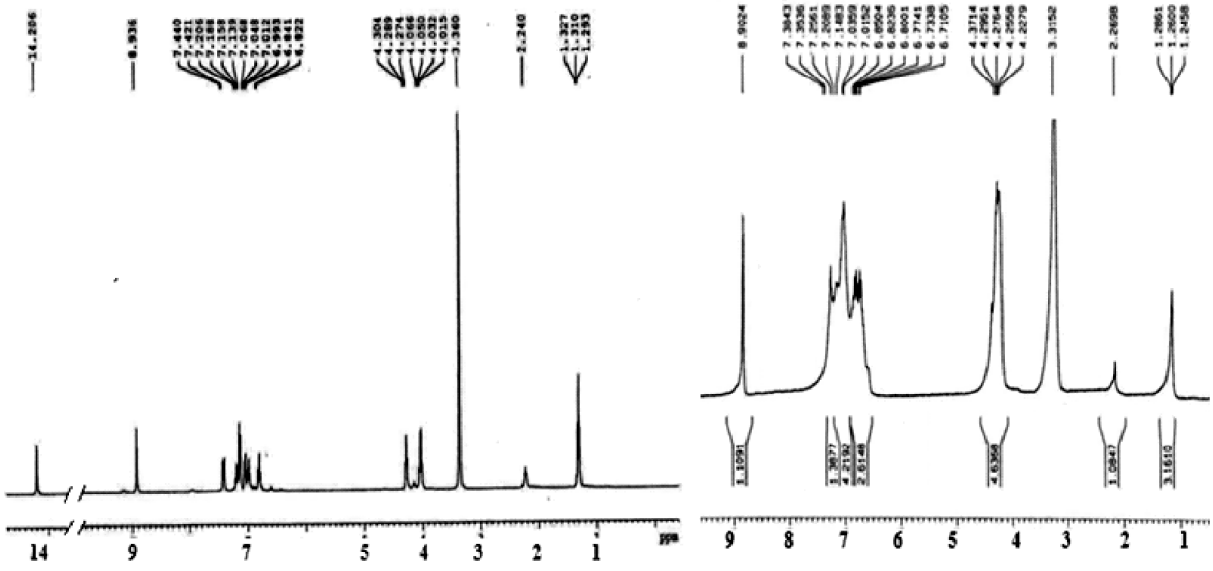

Fig. 1. ^{1}H NMR spectrum of (a) **H_2L** and (b) [Zn**L**] in DMSO-d_6.

The fluorescence quantum yield was determined taking fluorescein as a reference with known quantum yield (ϕ_R= 0.79 in 0.1 *M* NaOH). The experimental sample and reference were excited at same wavelength, maintaining almost same absorbance in the UV spectra. Area of the fluorescence spectra were measured using the software available in the instrument and the quantum yield was calculated by using the following formula:

$$\frac{\phi_S}{\phi_R} = \left[\frac{A_S}{A_R}\right] \times \left[\frac{(Abs)_R}{(Abs)_S}\right] \times \left[\frac{\eta_S^2}{\eta_R^2}\right]$$

where, ϕ_S and ϕ_R are the fluorescence quantum yield of the samples and reference. A_S and A_R are the areas under the emission spectra of the sample and reference respectively. $(Abs)_R$, $(Abs)_S$ are the absorbance of reference and sample at the excitation wave length. η_S^2, η_R^2 are the refractive index of the solvent used for the sample and the reference.

Theoretical calculation

DFT/B3LYP protocol was adopted using Gaussian 09 software to optimize the structures of **H_2L** and [Zn**L**][26,27]. 6-311G basis set was used for C, H, N, and O while LanL2DZ basis set was designated as effective core potential for Zn. The optimization was established by the calculation of vibrational frequency with local minima which only generated positive Eigen values. UV-Vis spectral transitions were calculated by time-dependent density functional theory (TD-DFT) method in acetonitrile solution using conductor-like polarizable continuum model (CPCM)[28,29]. GAUSSSUM was used for the calculation of the fractional contributions of various groups to each molecular function[30].

Results and discussion

Synthesis and formulation

6,6′-((1Z,1′Z)-(((Propane-1,3-diylbis(oxy))bis(2,1-phenylene))bis(azanylylidene))bis-(methanylylidene))bis(2-ethoxyphenol) (**H_2L**) is used (Scheme 1) in this work. The ^{1}H NMR spectrum shows phenolic-OH signal as singlet at 14.20 ppm and imine-H appears at 8.93 ppm (singlet); other characteristic signals are δ (-$\underline{CH_2}$-CH_2-$\underline{CH_2}$-), 4.28; δ (-O$\underline{CH_2}$-CH_3), 4.04; δ (-CH_2-$\underline{CH_2}$-CH_2-), 2.24; δ (-OCH_2-$\underline{CH_3}$), 1.31 ppm and other aromatic-Hs appear at 6.82–7.44 ppm (Fig. 1). Mass ion peak of **H_2L** appears at 555.27 which corresponds to calculated mass of (**H_2L** + H)$^+$ (ESI†, Fig. S2). The IR spectrum shows ν(C=N) at 1619 cm^{-1} and ν(phenolic-OH) at 3370 cm^{-1} (ESI†, Fig. S3).

UV-Vis and fluorescence spectroscopic studies

The UV-Vis absorption spectrum of the probe, **H_2L** in 9:1 (v/v) CH_3CN/H_2O (HEPES buffer, pH 7.4) shows absorption band at 340 nm which may due to and π-π* transition. Upon addition of Zn^{2+} to **H_2L** solution the absorbance at 340 nm decreases and a new band appears at 402 nm along with two isobestic points at 323 and 380 nm until 1:1 stoichiometry is reached (Fig. 2). The above spectral change indicates

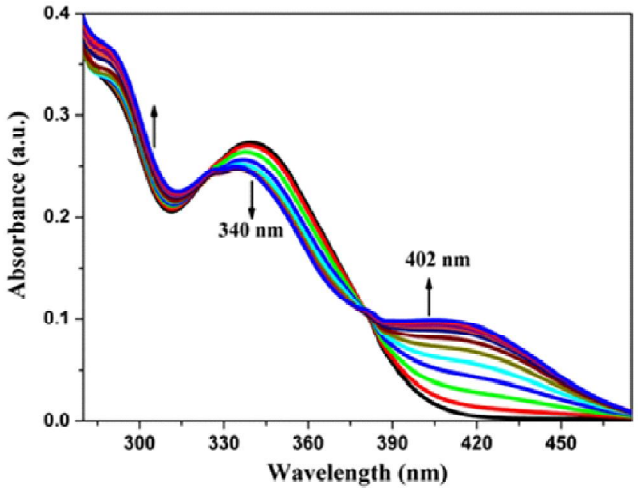

Fig. 2. Absorption spectral change of the probe, $\mathbf{H_2L}$ (50 μM) upon gradual addition of Zn^{2+} ion (0–50 μM) in 9:1 CH_3CN/H_2O v/v (10 μM HEPES buffer, pH 7.4).

that there may be formation of coordination complex of $\mathbf{H_2L}$ with Zn^{2+} ion and the change in absorbance may be due to intra-ligand-charge transfer (ILCT) transition.

The free probe, $\mathbf{H_2L}$ is non-emissive (λ_{ex}, 400 nm). Fluorescence spectra of $\mathbf{H_2L}$ have been recorded in presence of different cations (Cr^{3+}, Fe^{3+}, Ni^{2+}, Cd^{2+}, Hg^{2+}, K^+, Co^{2+}, Cu^{2+}, Pd^{2+}, Mn^{2+}, Mg^{2+}, Al^{3+}, Zn^{2+}, Pb^{2+}, Na^+, Ca^{2+} and Ba^{2+}) in 9:1 (v/v) CH_3CN/H_2O (HEPES buffer, pH 7.4) (Fig. 3). No significant fluorescence spectral change of the probe, $\mathbf{H_2L}$ is

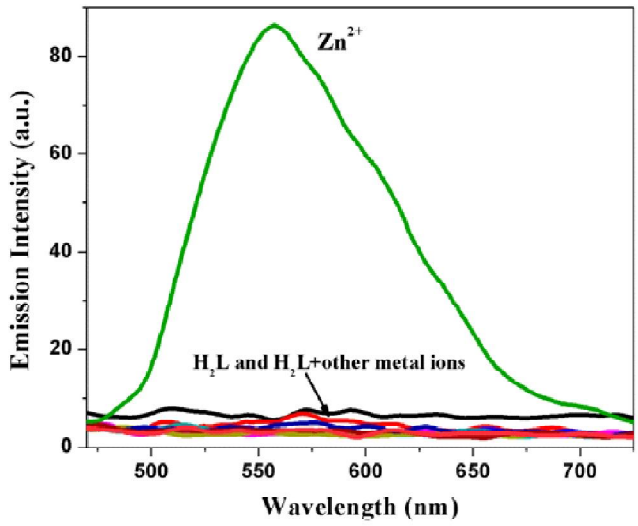

Fig. 3. Fluorescence spectra of the probe, $\mathbf{H_2L}$ (50 μM) upon gradual addition of different metal ions (50 μM) in 9:1 CH_3CN/H_2O v/v (10 mM HEPES buffer, pH 7.4), λ_{ex}, 400 nm.

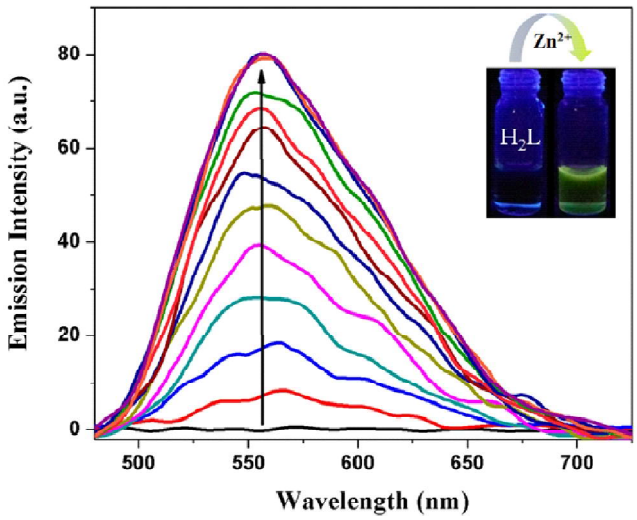

Fig. 4. Emission spectral change of the probe, $\mathbf{H_2L}$ (50 μM) upon gradual addition of Zn^{2+} ion (50 μM) in 9:1 CH_3CN/H_2O v/v (10 mM HEPES buffer, pH 7.4), λ_{ex}, 400 nm; inset: vial images in absence and presence of Zn^{2+} ions under UV chamber (λ, 365 nm).

observed except Zn^{2+} ion. Upon gradual addition of Zn^{2+} ion into the $\mathbf{H_2L}$ solution emission intensity at 556 nm increases continuously (~203 times enhancement with respect to free probe) till probe:metal stoichiometry reached to 1:1 (Fig. 4).

The emission intensity at 556 nm increases and the quantum yield is also enhanced by ~27 fold compared to free probe ($\phi_{[H_2L]} = 0.0009$ and $\phi_{[ZnL]} = 0.024$). The limit of detection (LOD) for Zn^{2+} ion is 15.5 nM, calculated by 3 σ/m method which is admirable than that of other previously reported Zn^{2+} ion sensor (ESI†, Fig. S6 and Table S1). $[(F_{max} - F_0)/(F - F_0)]$ vs $1/[Zn^{2+}]$, Benesi-Hildebrand equation has been used to calculate the binding constant between $\mathbf{H_2L}$ and Zn^{2+} ion and its value is 4.3×10^4 M^{-1} (ESI†, Fig. S7). The variation of emission intensity of $\mathbf{H_2L}$ for Zn^{2+} sensing upon pH has also been studied; the probe itself is non-emissive throughout the pH range 2–12 but $\mathbf{H_2L}$-Zn^{2+} shows emission in the pH range 8 to 12 (Fig. 5). The interference of various metal ions (other than Zn^{2+}) in the fluorescence of Zn^{2+} complex has also been studied in presence of other sixteen metal ions which shows significant fluorescence sensitivity of $\mathbf{H_2L}$ towards Zn^{2+} in which other ions co-exits (Fig. 6). A small interference is observed in presence of Fe^{3+} and Cu^{2+} ion due to paramagnetic quenching effect.

In order to clarify the nature of the binding mode and stoichiometry of $\mathbf{H_2L}$ to Zn^{2+}, the ^1H NMR spectrum of $\mathbf{H_2L}$

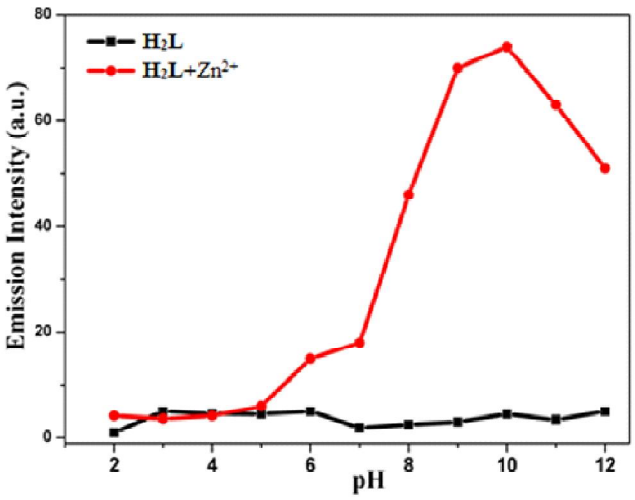

Fig. 5. Fluorescence intensity at different pH of the probe **H_2L** (20 μM) in the absence and presence of Zn^{2+} (20 μM) in 9:1 CH_3CN/H_2O mixture, $\lambda_{ex,}$ 400 nm.

has been investigated in absence and in presence of Zn^{2+} ion in DMSO-d_6 (Fig. 1). The ^{1}H NMR spectrum of [Zn**L**] shows the removal of singlet signal at 14.20 ppm corresponds to δ(phenolic-OH) from **H_2L** and the imine proton signal δ(H-C=N) has been shifted to upfield from 8.93 to 8.90 ppm. In the free probe, **H_2L** the aromatic protons were at 6.82–7.44 ppm and upon complexation with Zn^{2+}, these protons are at 6.71–7.38 ppm. The ^{1}H NMR signal movement favours the chemical interaction of Zn^{2+} with **H_2L** (Scheme 2). Job's plot for the reaction between **H_2L** and Zn^{2+} in CH_3CN-water (9:1, v/v) also supports the 1:1 complex formation (ESI†, Fig. S8). ESI-MS spectrum of **H_2L**-Zn^{2+} complex was appeared at 617.22 which corresponds to Zn**L** + H^+ ion (*m/z* Calcd. 617.15) and a base peak at 639.20 indicates Zn**L** + Na^+ ion (*m/z* Calcd. 639.14) which also proves the formation of 1:1 complex (ESI†, Fig. S4). The average lifetime of [Zn**L**] complex (0.766 ns) is increased than that of the free probe, **H_2L**

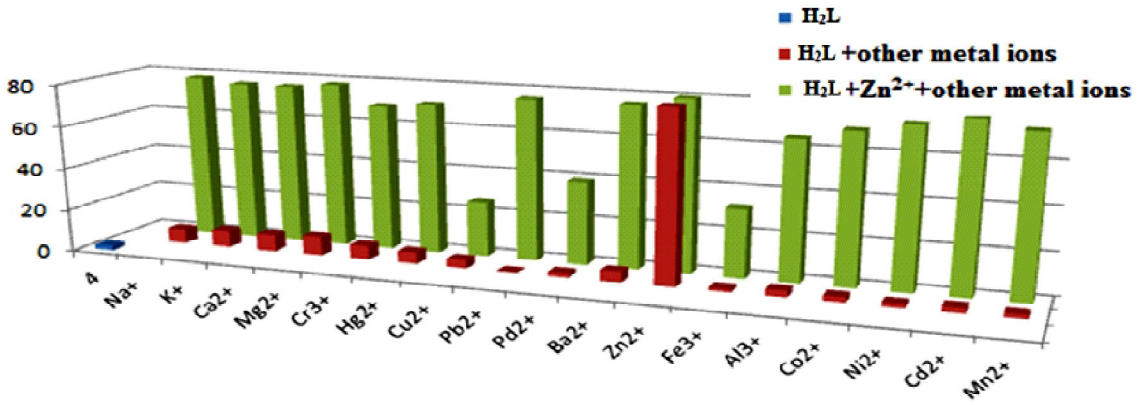

Fig. 6. Interference of metal ions on Zn^{2+} sensitivity in 9:1 CH_3CN/H_2O mixture.

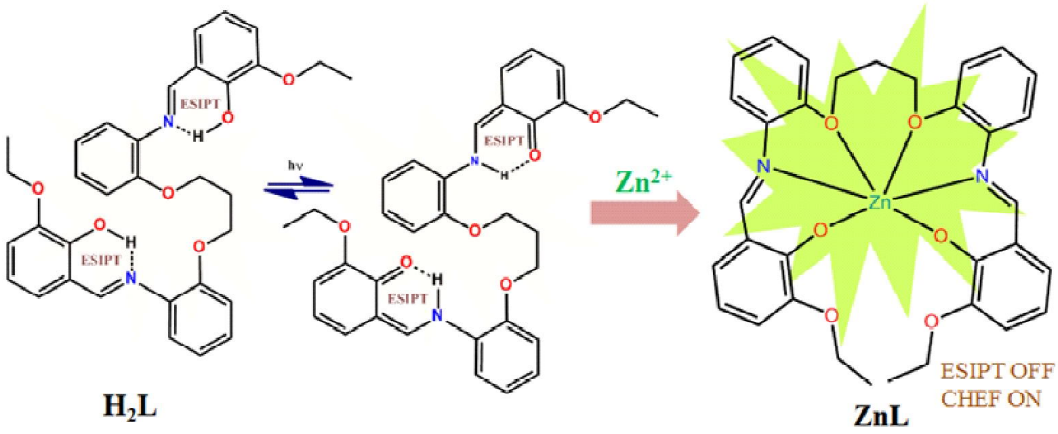

Scheme 2. Proposed sensing mechanism of **H_2L** with Zn^{2+}.

(t_{av}, 0.656 ns) (ESI†, Fig. S9) which may due to the metal-ligand orbital mixing of delocalised 3d π orbital of Zn^{2+} and π* of **H_2L** in the excited state.

Density functional theory calculation

Density Functional Theory (DFT) calculations are taken by B3LYP/6-311G method and basis set in the Gaussian 09 software for optimization of the probe, **H_2L** and its zinc complex (ESI†, Fig. S10). Some frontier molecular orbitals with energy of **H_2L** and [Zn**L**] complex are also listed (ESI†, Figs. S11 and S12). The band gap of HOMO and LUMO of the probe **H_2L** and Zn**L** are shown in Fig. 7. The HOMO-LUMO energy gap is found to be 4.00 eV and 2.51 eV for **H_2L** and [Zn**L**] complex respectively which indicates decrease in band gap upon complexation. By using the time dependent density functional theory (TD-DFT) with CPCM method (in CH_3CN medium), the ground state electronic spectra both for **H_2L** and [Zn**L**] complexes were calculated. For the probe **H_2L**, the absorption a maximum at 340 nm is mainly due to HOMO-1→LUMO+1 transition (ESI†, Table S2). For [Zn**L**] complex the transition from HOMO→LUMO+1 and HOMO-3→LUMO have contributions mainly due to the absorption bands at 402 and 340 nm respectively (ESI†, Table S3). The absorption wavelength found from DFT calculations are well matched with the peaks obtained experimentally and support the red shifting absorption upon complexation with Zn^{2+} ion.

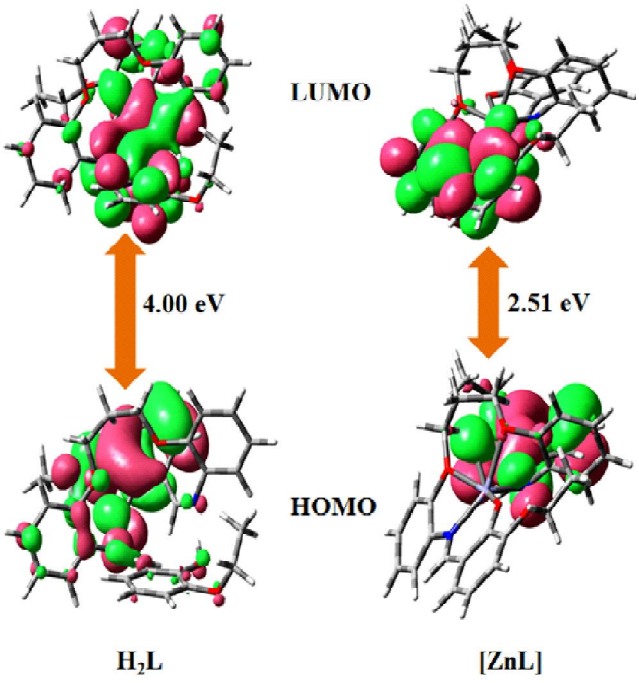

Fig. 7. HOMO-LUMO band gap of **H_2L** and [Zn**L**] complex.

Conclusion

We have synthesized and characterized a Schiff base, 6,6′-((1Z,1′Z)-(((propane-1,3-diylbis(oxy))bis(2,1-phenylene))bis(azanylylidene))bis-(methanylylidene))bis(2-ethoxyphenol), (**H_2L**) by using condensation method (2,2′-(propane-1,2-diylbis(oxy))dianiline with 3-ethoxy-2-hydroxybenzaldehyde). Zn^{2+} has been selected by probe **H_2L** spectrophotometrically via Chelation Enhanced Fluorescence (CHEF) with LOD, 15.5 nM in CH_3CN/H_2O (v/v 9:1, HEPES buffer, pH 7.4). A high intense greenish yellow emission is observed at 556 nm wavelength. So, from the above discussed observation we can conclude that the synthesized probe is highly selective for Zn^{2+} ion with very low limit of detection.

Acknowledgement

For providing financial support from the Council of Scientific and Industrial Research (CSIR, Sanction no. 01(2894)/09/EMR-II), New Delhi, India is thankfully acknowledged. One of our co-authors (SD) is also grateful to Council of Scientific and Industrial Research, Govt. of India for providing CSIR-research fellowship. CS thanks RUSA 2.0 for financial help.

References

1. Z. Xu, J. Yoon and D. R. Spring, *Chem. Soc. Rev.*, 2010, **39**, 1996.
2. B. L. Vallee and K. H. Falchuk, *Physiol. Rev.*, 1993, **73**, 79.
3. J. M. Berg and Y. Shi, *Science*, 1996, **271**, 1081.
4. D. T. Quang and J. S. Kim, *Chem. Rev.*, 2010, **110**, 6280.
5. X. Chen, T. Pradhan, F. Wang, J. S. Kim and J. Yoon, *Chem. Rev.*, 2012, **112**, 1910.
6. X. Xie and T. G. Smart, *Nature*, 1991, **349**, 521.
7. P. Jiang and Z. Guo, *Coord. Chem. Rev.*, 2004, **248**, 205.
8. H. Y. Lin, P. Y. Cheng, C. F. Wan and A. T. Wu, *Analyst*, 2012, **137**, 4415.
9. R. Parkesh, T. C. Lee, T. Gunnlaugsson, *Org. Biomol. Chem.*, 2007, **5**, 310.
10. M. S. Park, K. M. K. Swamy, Y. J. Lee, H. N. Lee, Y. J. Jang, Y. H. Moon and J. Yoon, *Tetrahedron Lett.*, 2006, **47**, 8129.
11. A. I. Bush, W. H. Pettingell, G. Malthaup, M. D. Paradis, J. P. Vonsattel, J. F. Gusella, K. Beyreuther, C. L. Masters and R. E. Tanzi, *Science*, 1994, **265**, 1464.
12. J. Y. Koh, S. W. Suh, B. J. Gwag, Y. Y. He, C. Y. Hsu and D. W. Choi, *Science*, 1996, **272**, 1013.

13. C. J. Frederickson, M. D. Hernandez and J. F. McGinty, *Brain Res.*, 1989, **480**, 317.
14. U. S. Environmental Protection Agency. Risk Assessment, Management and Communication of Drinking Water Contamination; US EPA 625/4-89/024, EPA: Washington, DC,1989.
15. T. Tulchinsky, MD, MPH, Public Health Reviews, 2010, **32**, 243.
16. A. Baran, *Pol. J. Environ. Stud.*, 2013, **22**, 77.
17. A. P. S. Gonzales, M. A. Firmino, C. S. Nomura, F. R. P. Rocha, P. V. Oliveira and I. Gaubeur, *Anal. Chim. Acta*, 2009, **636**, 198.
18. C. Shi, S. Xie and J. Jia, *J. Autom. Methods Manage. Chem.*, 2008, **2008**, 453429.
19. Y. Liu, P. Liang and L. Guo, *Talanta*, 2005, **68**, 25.
20. J. Zhanga, B. Zhaoa, C. Lia, X. Zhub and R. Qiao, *Sens. Actuators B*, 2014, **196**, 117.
21. C. Chen, D. Liao, C. Wan and A. Wu, *Analyst*, 2013, **138**, 2527.
22. Y. Choi, G. Park, Y. Na, H. Jo, S. Lee, G. You and C. Kim, *Sens. Actuators B*, 2014, **194**, 343.
23. A. Kumar, A. Kumar and D. Pandey, *Dalton Trans.*, 2016, **45**, 8475.
24. K. Aich, S. Goswami, S. Das and C. D. Mukhopadhyay, *RSC Adv.*, 2015, **5**, 31189.
25. B. S. Furniss, A. J. Hannaford, P. W. G. Smith and A. R. Tatchell, "Vogel's Text Book of Practical Organic Chemistry", 5th ed., John Wiley & Sons, Inc., New York, 1989.
26. M. J. Frisch, G. W. Trucks, H. B. Schlegel, G. E. Scuseria, M. A. Robb, J. R. Cheeseman, G. Scalmani, V. Barone, B. Mennucci, G. A. Petersson, H. Nakatsuji, M. Caricato, X. Li, H. P. Hratchian, A. F. Izmaylov, J. Bloino, G. Zheng, J. L. Sonnenberg, M. Hada, M. Ehara, K. Toyota, R. Fukuda, J. Hasegawa, M. Ishida, T. Nakajima, Y. Honda, O. Kitao, H. Nakai, T. Vreven, J. A. Montgomery (Jr.), J. E. Peralta, F. Ogliaro, M. Bearpark, J. J. Heyd, E. Brothers, K. N. Kudin, V. N. Staroverov, R. Kobayashi, J. Normand, K. Raghavachari, A. Rendell, J. C. Burant, S. S. Iyengar, J. Tomasi, M. Cossi, N. Rega, J. M. Millam, M. Klene, J. E. Knox, J. B. Cross, V. Bakken, C. Adamo, J. Jaramillo, R. Gomperts, R. E. Stratmann, O. Yazyev, A. J. Austin, R. Cammi, C. Pomelli, J. W. Ochterski, R. L. Martin, K. Morokuma, V. G. Zakrzewski, G. A. Voth, P. Salvador, J. J. Dannenberg, S. Dapprich, A. D. Daniels, O. Farkas, J. B. Foresman, J. V. Ortiz, J. Cioslowski, D. J. Fox, Gaussian 09, Revision D.01, Gaussian Inc, Wallingford, CT, 2009.
27. A. D. Becke, *J. Chem. Phys.*, 1993, **98**, 5648.
28. M. Cossi and V. Barone, *J. Chem. Phys.*, 2001, **115**, 4708.
29. M. Cossi, N. Rega, G. Scalmani and V. Barone, *J. Comput. Chem.*, 2003, **24**, 669.
30. N. M. O'Boyle, A. L. Tenderholt and K. M. Langner, *J. Comput. Chem.*, 2008, **29**, 839.